Polymer Chemistry

ROYAL SOCIETY OF CHEMISTRY

PAPER

View Article Online
View Journal | View Issue

Cite this: *Polym. Chem.*, 2025, **16**, 3511

Tunable adhesion properties of hydrolytically degradable aliphatic polyester triblock/diblock copolymer blends†

Shuang Liang, [a] Christopher J. Ellison *[b] and Marc A. Hillmyer *[a]

Tuning the molecular architecture of block copolymer blends is a powerful strategy to optimize their performance in pressure-sensitive adhesive (PSA) formulations. To improve the sustainability of typical petroleum derived and non-degradable PSAs, aliphatic polyester block copolymer blends of poly(L-lactide)-*block*-poly(γ-methyl-ε-caprolactone)-*block*-poly(L-lactide) (LML) and poly(L-lactide)-*block*-poly(γ-methyl-ε-caprolactone) (ML) were prepared by combining sequential ring-opening transesterification polymerization and copper-catalyzed alkyne–azido cycloaddition reaction. We systematically investigated the effects of blend compositions on their microstructural, thermal, mechanical, and adhesion properties in PSA formulations that included tackifier. Using optimized triblock content and thermal annealing protocols, the tackified PSAs exhibited competitive adhesion properties when compared to established styrenic PSAs. For example, a PSA of LML/ML (mass ratio = 1 : 1) with 20 wt% tackifier showed a peel strength of 3.66 ± 0.33 N cm^{-1}, a shear resistance of 429 ± 62 min and a desired adhesive failure mode. The competitive adhesion performance is attributed to a balance between dangling and bridging PγMCL end- and mid-blocks in the rubbery matrix that simultaneously allows interfacial adhesion and cohesive strength for favorable PSA bonding and debonding. The LML/ML-based PSAs are hydrolytically degradable into water soluble or dispersible compounds at 45 °C under basic conditions within 25 days. Our results indicate rationally tailoring the molecular architecture of polyester block copolymer blends is a convenient and robust strategy to optimize their adhesion properties for sustainable PSA solutions.

Received 21st May 2025,
Accepted 26th June 2025

DOI: 10.1039/d5py00506j

rsc.li/polymers

Introduction

Pressure-sensitive adhesives (PSAs) are soft solids that combine rapid substrate adhesion under light pressure, effective stress resistance once adhered, and clean removability without residue.[1–3] Ideal PSAs have complementary properties of viscous liquids and elastic solids, which necessitate precise design and engineering of their molecular characteristics, compositions, formulations, and processing techniques.[4–7] Among contemporary PSAs, tackified styrenic copolymers with a microphase-separated ABA triblock architecture are of particular interest due to their tunable mechanical properties and cost-effectiveness.[8–10] Styrenic ABA triblocks are typically comprised of 10–30 weight percent (wt%) glassy/minority "A" polystyrene (PS) blocks with the remainder being a chemically incompatible rubbery/majority "B" midblock (*e.g.*, polyisoprene (PI) or polybutadiene (PB)) with a glass-transition temperature (T_g) well below room temperature.[8,10] The rubbery "B" midblock forms a soft matrix to allow efficient interfacial adhesion and glassy, microphase-separated PS domains that act as physical cross-links to provide cohesive strength and creep resistance under stress.[2] Blending tackifier that is chemically compatible with the rubbery midblock matrix results in selective midblock domain swelling. As a result, midblock entanglements are effectively diluted which promotes substrate adhesion.[11] These properties provide styrenic block copolymer-based blends with necessary adhesion properties for use in a wide range of applications, such as in tapes and labels.[1,12]

Blending PS-*block*-PI-*block*-PS (SIS) triblocks with PS-*block*-PI (SI) diblocks is a convenient and robust strategy to optimize mechanical properties and adhesion performance of PSAs.[10,13–15] Compared to pure SIS or SI, previous work has shown that SIS/SI blends with 75 wt% SI diblock exhibited a significant increase in probe tack force and enhanced

[a]*Department of Chemistry, University of Minnesota, Minneapolis, Minnesota, 55455, USA. E-mail: hillmyer@umn.edu*
[b]*Department of Chemical Engineering and Materials Science, University of Minnesota, Minneapolis, Minnesota, 55455, USA. E-mail: cellison@umn.edu*

†Electronic supplementary information (ESI) available: Materials, additional experimental details, supplementary characterization data (^{1}H NMR, SEC, and Rheology), adhesion test and hydrolytic degradation data. See DOI: https://doi.org/10.1039/d5py00506j

peel strength (the force per unit width required to debond a PSA from its substrate).[16] In this case, the SI diblock copolymer components were approximately half the molar mass of their SIS triblock analogs, while maintaining similar PS content. While the linear viscoelastic properties were comparable,[10] the progressive addition of SI diblock copolymer into the SIS/SI blends increased dangling PI ends in the rubbery matrix. Consequently, the enhanced dissipative properties and molecular mobility allowed more efficient interfacial substrate adhesion.[4,16] In contrast, the peel strength is heavily dependent upon nonlinear mechanical properties at large-strains.[3] Implementing rubbery PI bridging chains between hard PS domains in SIS triblocks increases the PSA cohesive strength, allowing for effective fibril formation and elongation during PSA debonding.[14,15] As a result, the primary debonding mechanism is adhesive failure, which is preferred over cohesive failure that generally leaves unwanted residue on the substrate. Optimizing the SIS/SI ratios in the blend enables convenient manipulation of the relative amounts of dangling PI ends from SI diblocks and bridging PI chains from SIS triblocks in the rubbery matrix, which can be used to balance the interfacial adhesion and cohesive strength.

Unfortunately, styrenic block copolymers are petroleum-derived with poor degradability, primarily owing to their all carbon–carbon bond backbones, which contributes to an unsustainable life cycle and plastic waste accumulation.[17] Significant efforts have been devoted to develop more sustainable alternatives, such as aliphatic polyester block copolymers, with comparable performance in PSA formulations.[18–20] The unique advantages of aliphatic polyester block copolymers come from their degradability under various conditions and the fact that they can often be sourced from renewable feedstocks. For instance, the γ-methyl-ε-caprolactone and L-lactide monomers of poly(L-lactide)-*block*-poly(γ-methyl-ε-caprolactone)-*block*-poly(L-lactide) (LML) triblocks can be produced from renewable resources.[21,22] Moreover, LMLs can be readily degraded *via* enzymatic hydrolysis or under simulated industrial composting conditions.[23,24] Therefore, poly(lactide)-*block*-poly(menthide)-*block*-poly(lactide),[25] poly(lactide)-*block*-poly(β-methyl-δ-valerolactone)-*block*-poly(lactide),[5] poly(lactide)-*block*-poly(pentadecyl-caprolactone)-*block*-poly(lactide),[26] and other poly(alkyl-δ-lactone)-based polyester block copolymers[19] were shown to have attractive PSA properties with the added benefit of enhanced sustainability.

In our previous work,[27] tackified LML-based PSAs with semicrystalline poly(L-lactide) (PLLA) end blocks, showed competitive adhesion properties compared to commercial PSAs and are hydrolytic degradable. Inspired by previous efforts on SIS/SI blends and blends of poly(lactide-*co*-caprolactone) of different molar masses for improved adhesion performance,[28,29] we pursued tailored ratios of poly(γ-methyl-ε-caprolactone)-*block*-poly(L-lactide) (ML) diblocks and LML triblocks in tackified PSA formulations. We explored effects of blend composition on the thermal, microstructural, mechanical, and adhesion properties.

Here we report the synthesis of a set of LML/ML blends with tunable ratios by combining sequential ring-opening transesterification polymerization (ROTEP) and copper-catalyzed alkyne–azido cycloaddition to produce the two components. The impacts of the LML wt% were probed by evaluating the thermal, microstructural, linear viscoelastic and tensile properties of blends after solvent-casting. The LML/ML blends were mixed with a rosin ester tackifier to swell the poly(γ-methyl-ε-caprolactone) (PγMCL) rubbery matrix and evaluated as degradable PSAs. The formulated PSAs from tackified LML/ML blends with optimized LML content were also prepared by two different methods to demonstrate the generalizability of this approach. To further improve the adhesion properties, the PSAs with optimized formulations were subjected to a two-step annealing process after solvent casting. Compared to tackified LML-based PSAs, the tackified LML/ML blend-based PSAs exhibited tunable and substantially improved peel adhesion properties, with shear resistance values comparable to commercial products.

Results and discussion

Synthesis and molecular characterizations

We synthesized end group functionalized ML by ROTEP (Scheme 1) and then coupled the reactive ML samples with a bifunctional linker to form LML/ML blends using a copper-catalyzed alkyne–azido cycloaddition reaction. Using literature procedures,[30,31] PγMCL was first synthesized by $Sn(Oct)_2$-catalyzed ROTEP in the melt at 130 °C for 90 min to reach high (>95%) monomer conversion using an alkyne-functionalized alcohol 3-butyn-1-ol as initiator. The as-prepared alkyne-terminated PγMCL had a total number average molar mass (M_n) of 33.1 kg mol^{-1}, determined by performing end-group analysis with proton nuclear magnetic resonance (^{1}H NMR) spectroscopy. The alkyne-terminated PγMCL with a hydroxyl end was used as a macroinitiator for the $Sn(Oct)_2$-catalyzed ROTEP of L-lactide at 130 °C for 90 min in toluene. The as-prepared alkyne-ML diblock copolymers were purified following previous work[31] and characterized by ^{1}H NMR spectroscopy (Fig. S1 and S2†) and size exclusion chromatography (SEC) (Fig. S3†). The SEC trace of alkyne-ML showed a clear shift in the elution time compared to that of its PγMCL precursor, while the ^{1}H NMR spectra also indicated a shift of the methylene terminal resonance from 3.7 ppm of PγMCL to 4.4 ppm of PLLA,[31] supporting the successful preparation of ML diblock copolymers. The alkyne terminus of ML diblock copolymers was validated by the presence of a peak around 1.95 ppm in the ^{1}H NMR spectra (Fig. 1). The alkyne-terminated ML diblock copolymer, denoted alkyne-ML(38.8, 0.26), had a total M_n of 38.8 kg mol^{-1}, dispersity ($Đ$) of 1.56, and a PLLA volume fraction (f_{PLLA}) of 0.26, which is similar to that of PLLA or PS hard blocks in previously reported block copolymers used in PSAs.[6,13,32]

The copper-catalyzed alkyne–azido cycloaddition reaction has been shown to be useful for modifying the molecular

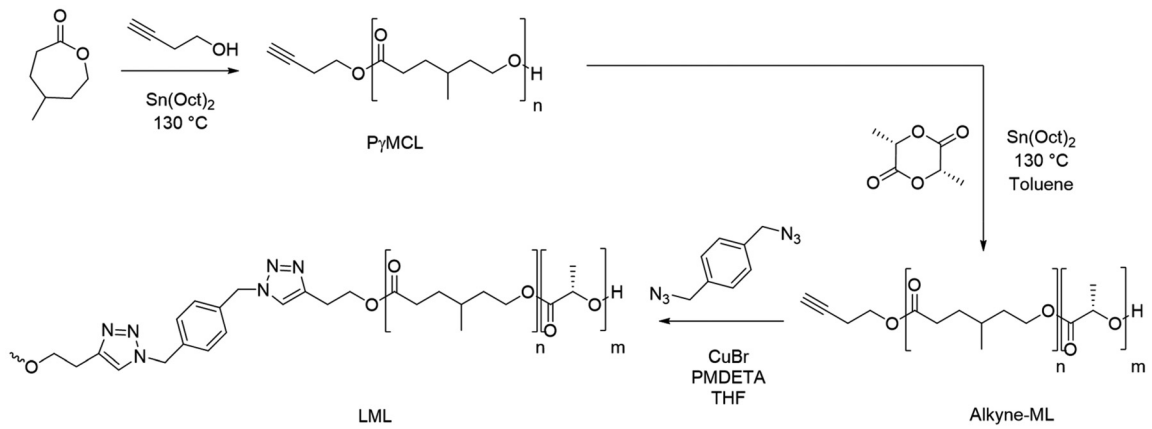

Scheme 1 Synthesis of alkyne-terminated PγMCL, alkyne-terminated poly(L-lactide)-*block*-poly(γ-methyl-ε-caprolactone) (alkyne-ML), and LML.

architecture of polyesters.[33–35] Following a literature procedure,[36] a bifunctional linker, α,α′-diazido-*p*-xylene, was synthesized, characterized *via* ^{1}H NMR spectroscopy (Fig. S4†). The bifunctional α,α′-diazido-*p*-xylene can be used to link two alkyne-ML(38.8, 0.26) diblock copolymers and form a LML triblock. The alkyne–azido cycloaddition reactions were executed in tetrahydrofuran (THF) at room temperature without light exposure, and catalyzed by CuBr for 24 h. The ligand *N*,*N*,*N*′,*N*′,*N*″-pentamethyldiethylenetriamine (PMDETA) was used to improve the solubility and reactivity of CuBr in THF. After purification (details in ESI†), ^{1}H NMR spectroscopic (Fig. 1) and SEC (Fig. 2) analyses corroborated the successful synthesis of the LML triblock architecture with commensurate arm length and f_{PLLA} as the ML diblock precursors.

All ^{1}H NMR spectra of LML/ML blends showed a substantial reduction in alkyne end group intensity (1.95 ppm) and emergence of new methylene hydrogens at 5.5 ppm and 2.8 ppm. The similar peak integration areas of these two distinctive methylene resonances indicated both azido ends on the linker had reacted with alkyne groups on ML(38.8, 0.26), suggesting successful LML formation. The LML wt% in the as-formed blends can be readily adjusted by tuning the alkyne-to-azido molar ratio, and this wt% was characterized by comparing peak integration areas of hydroxyl termination resonance at 2.65 ppm (ref. 37) and methylene resonances at 5.5 ppm. Full conversion of ML to LML would lead to an integration ratio of 1 to 2 and 100 wt% LML in the blend. For example, 50% conversion of alkyne groups would yield a 1 to 1 integration ratio of these two peaks (third trace from the bottom in Fig. 1). Since the as-formed LMLs have approximately twice the molar mass of pristine alkyne-ML(38.8, 0.26), 50% conversion of alkyne-ML (38.8, 0.26) would produce an LML/ML blend with 50 wt% LML. Three LML/ML blends were prepared with 25 wt% (second trace from the bottom in Fig. 1, denoted 25 wt% LML), 50 wt% (third trace from the bottom in Fig. 1, denoted 50 wt% LML), and 75 wt% (top trace in Fig. 1, denoted 75 wt% LML) LML, respectively. However, previous studies showed that the second ROTEP of L-lactide could also produce PLLA homopolymer alongside block copolymers if there is adventitious initiator present,[30,37] which may result in some error in determining (and very likely underestimating) the reaction conversion and LML wt% in the blends *via* ^{1}H NMR. The exchangeable protons on the hydroxyl terminations may also introduce errors in determining the LML to ML ratios. Theoretically, the methylene resonances at 5.5 ppm should be a singlet as shown in the pristine linker (Fig. S4†) and 25 wt% LML, rather than a doublet in 50 wt% and 75 wt% LML. The exact reason for this change of multiplicity is unknown, but may be a result of the formation of regioisomers.

Successful preparation of LML/ML blends was also confirmed *via* SEC analysis; all blends shifted to shorter elution times (Fig. 2), indicating a molar mass increase after ML-linking reactions (Table 1). While a bimodal SEC trace from a sample containing both LML triblock and ML diblock copolymers may be expected, the high dispersity of the starting alkyne-ML(38.8, 0.26) ($Đ$ = 1.56) resulted in the observation of a unimodal but broad shape in the respective blend SEC traces. While the molar masses of 25 wt% LML and 50 wt% LML blends followed expectation based on coupling conversion, the 75 wt% LML blend yielded a molar mass (81.6 kg mol^{-1}), slightly higher than the theoretical molar mass of fully converted alkyne-ML(*i.e.*, 77.6 kg mol^{-1}). While azido functionalized polyacrylates are known to cross-link and form networks *via* nitrene insertion into a C–H-containing backbone under UV light irradiation,[38] a control polymer sample was prepared without alkyne functionalization and reacted under these conditions, which confirmed no detectable nitrene insertion side reaction occurred (details in Table S1 and Fig. S5†). The slightly higher molar mass of the 75 wt% LML blend and narrowed SEC peak for the blend products compared to the alkyne-ML precursor may be a combined result from an underestimated amount of LML, error in SEC measurement, *e.g.*, due to small amounts of column interactions, and/or high dispersity of starting alkyne-ML(38.8, 0.26).

In the ^{1}H NMR spectrum of the 25 wt% LML blend, the peak intensity of the alkyne endgroup in the unreacted alkyne-

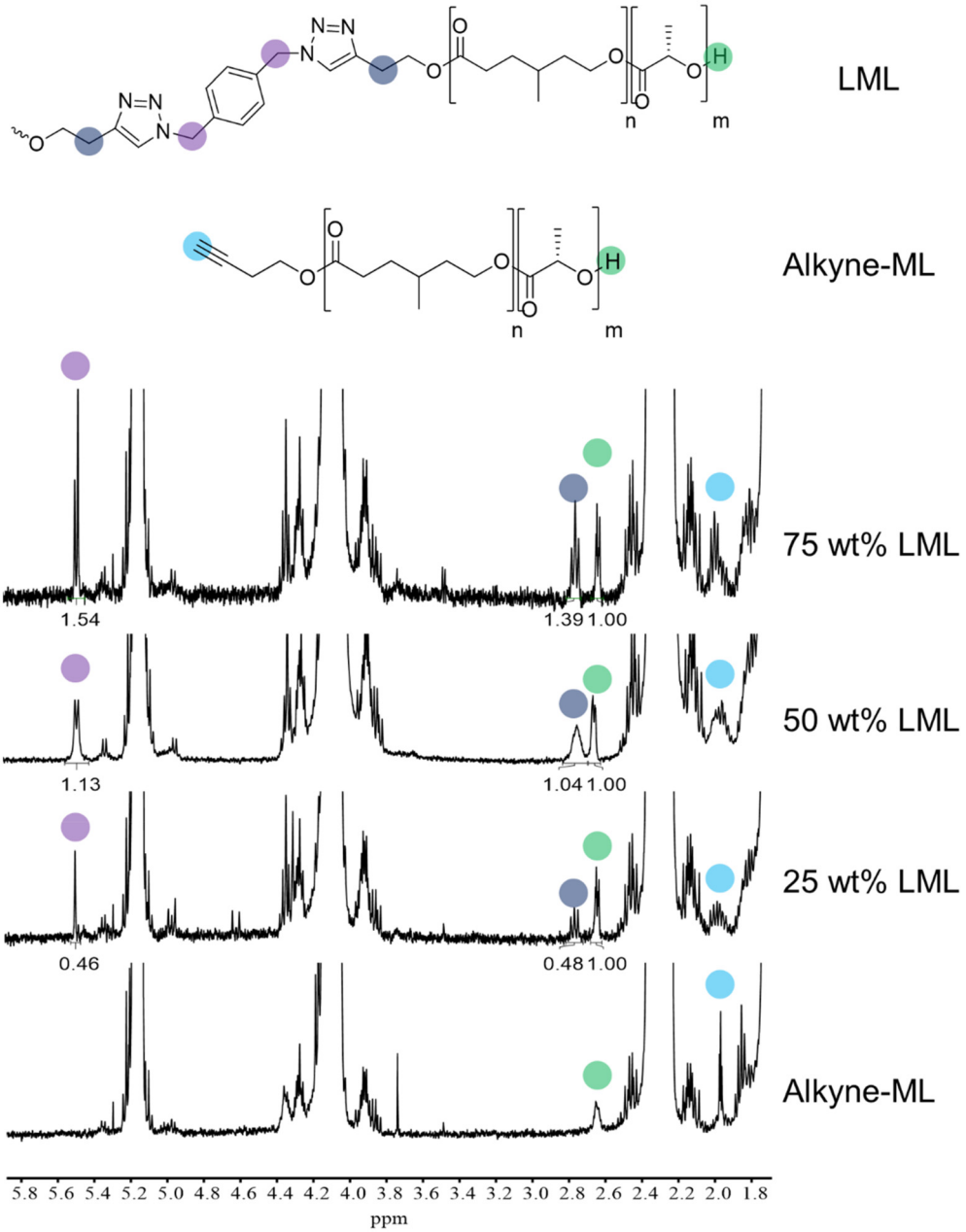

Fig. 1 ^{1}H NMR spectra of alkyne-ML and LML/ML blends.

ML diblock was much lower than expected based on the end-group analysis mentioned above. To verify if alkyne-ML(38.8, 0.26) with active alkyne endgroups remained in the blend, a small portion of 25 wt% LML blend was subjected to further reaction with excess α,α′-diazido-*p*-xylene bifunctional linker (molar ratio of azido to residual alkyne = 2 : 1) under the same conditions of initial copper-catalyzed alkyne–azido cycloaddition. Notably, SEC results (Fig. S6 and Table S2†) showed the molar mass of the 25 wt% LML blend could be further increased to 77.8 kg mol^{-1}, which is comparable to the theoretical molar mass for 100 wt% LML (77.6 kg mol^{-1}). This result suggests the alkyne terminations remained active in the blends with high residual ML content and further confirmed that the excess azido group does not participate significantly in unfavorable nitrene insertion side reactions.

Microstructural, thermal, linear viscoelastic and tensile properties

Before blending with tackifier and implementing as PSAs and to understand the impact of LML content, alkyne-ML(38.8, 0.26) and three LML/ML blends were solvent-cast from chloroform into 400 μm films (details in ESI†). Similar to previous work,[27] the small angle X-ray scattering (SAXS) patterns (Fig. 3) of pristine alkyne-ML(38.8, 0.26) and three LML/ML blends

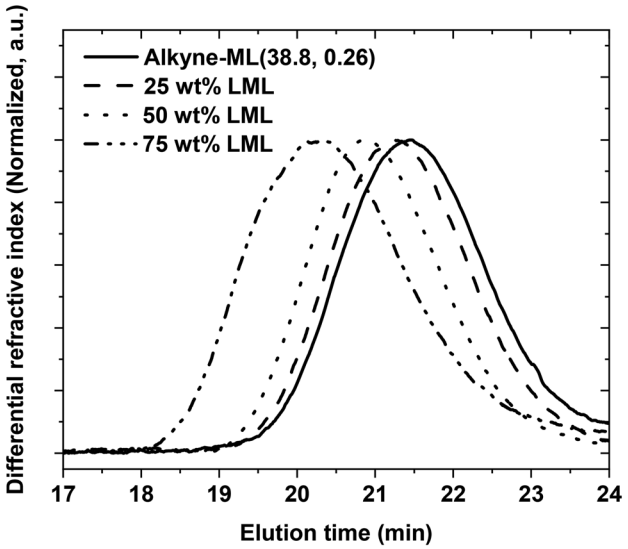

Fig. 2 THF-SEC traces of alkyne-ML(38.8, 0.26) and LML/ML blends.

Table 1 Molar mass and dispersity of the as-prepared alkyne-ML block copolymers and LML/ML blends

Sample ID ($M_{n,total}$, f_{PLA})	$M_{n,SEC,MALLS}$[a] (kg mol^{-1})	$Đ$[b]
Alkyne-ML(38.8, 0.26)	36.4	1.56
25 wt% LML	45.5	1.41
50 wt% LML	57.2	1.40
75 wt% LML	81.6	1.71

[a] Determined using THF-SEC with multi-angle laser light scattering (MALLS) detector. [b] Determined using THF-SEC with differential refractive index (RI) detector.

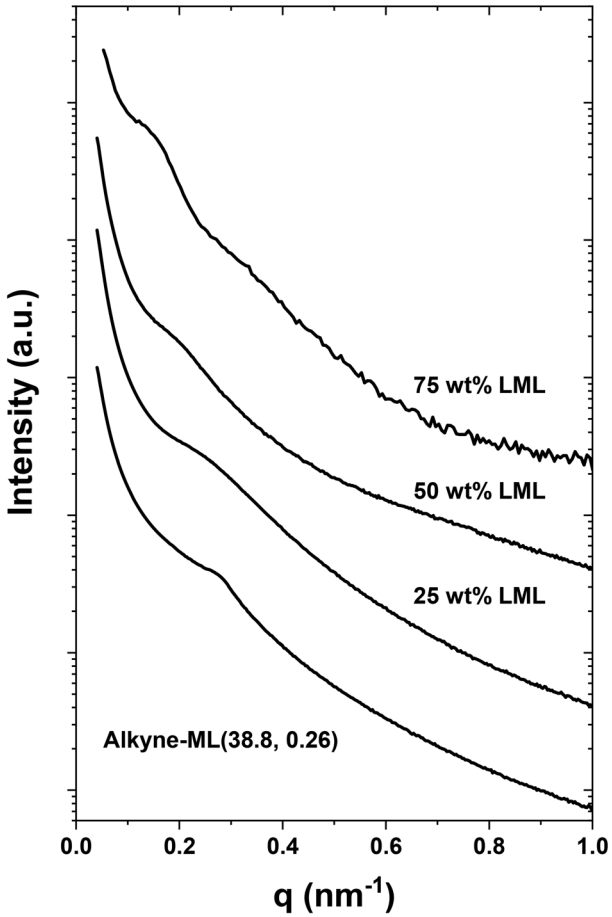

Fig. 3 SAXS patterns of alkyne-ML(38.8, 0.26) and LML/ML blends after solvent casting (vertically shifted for clarity).

showed broad principal scattering peaks and no higher-order peaks after solvent casting, suggesting some level of microphase separation without long-range order. The rapid chloroform evaporation during the solvent casting and drying process likely trapped the blends in a non-equilibrium state.[39] Similar scattering patterns observed in the alkyne-ML(38.8, 0.26) and three LML/ML blends highlights that the introduction of molecular linkage and bridging PγMCL chains in LML did not significantly impact the microphase separated morphology during solvent casting, which is similar to the case of poly(cyclohexylethylene)-*block*-poly(ethylene) multi-block polymer blends.[40] However, the principle domain spacing $D = 2\pi/q^*$ is 22.8 nm for alkyne-ML(38.8, 0.26) at room temperature, where q^* is the magnitude of the scattering vector at the primary peak. Since domain spacing is sensitive to molar mass and block architecture,[41] we expected formation of LML triblocks to lead to different domain spacings, evidenced by shifts to lower q^*-values. The formation of LML shifted q^* to lower values and increased domain spacing to 26.7 nm for 25 wt% LML blends, 31.9 nm for 50 wt% LML blends, and 38.8 nm for 75 wt% LML blends. These results corroborated the linking of alkyne-terminated ML diblock copolymers produced an LML triblock architecture in the blends with higher molar mass and longer chain length, which will contribute to more bridging PγMCL chains in the rubbery PγMCL matrix that connect to two PLLA hard domains.

The thermal properties were investigated by differential scanning calorimetry (DSC) (Fig. 4) and summarized in Table 2. After solvent casting, the first heating traces of alkyne-ML(38.8, 0.26) and LML/ML blends all showed a $T_{g,PγMCL} \approx -60$ °C, a $T_{g,\ PLLA}$ around 54–59 °C, and a $T_{m,PLLA}$ (melting temperature of semi-crystalline PLLA) centered around 160 °C, indicating the alkyne-ML(38.8, 0.26) and LML/ML blends shared similar thermal properties. The presence of T_g's for both block types supports microphase separation between PγMCL and PLLA blocks.[27,30,31] The degree of PLLA crystallinity remained low (*i.e.*, around 0.1 in Table 2) and was similar in all blends without a clear trend, which may be a result of formation of a non-equilibrium microstructure during rapid solvent evaporation. The appearance of an additional shoulder in the melting endotherms of alkyne-ML (38.8, 0.26) and 25 wt% LML traces may be attributed to the formation of smaller PLLA crystals or the presence of the α′-form of PLLA crystals, which normally have a lower melting temperature than the more stable α-form of PLLA crystals.[42]

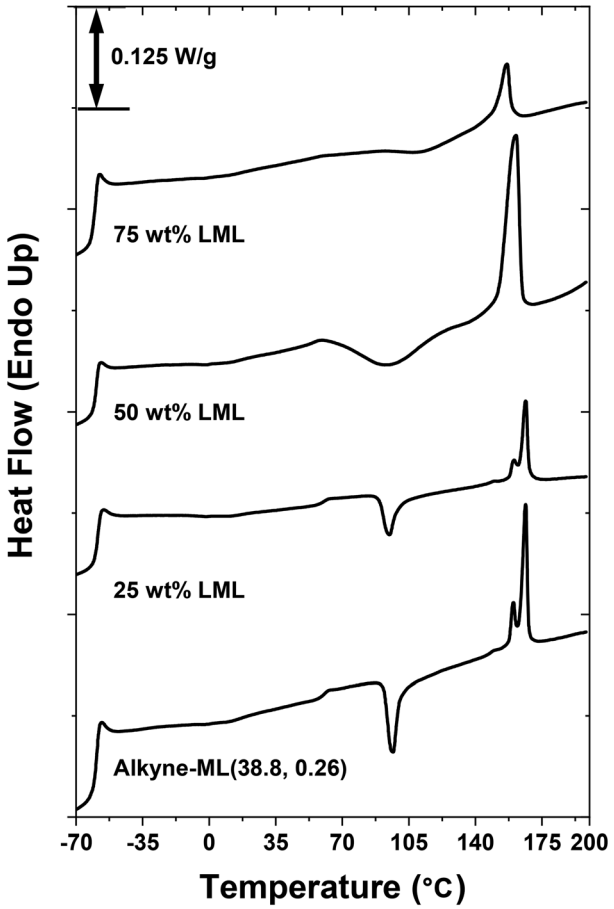

Fig. 4 DSC traces of alkyne-ML(38.8, 0.26) and LML/ML blends after solvent casting (first heating, 10 °C min^{-1}) (vertically shifted for clarity).

Table 2 Thermal properties of alkyne-ML(38.8, 0.26) and LML/ML blends after solvent casting

Sample ID	$T_{g,\ P\gamma MCL}$[a] (°C)	$T_{m,\ PLLA}$[b] (°C)	$T_{g,\ PLLA}$[a] (°C)	Degree of PLLA crystallinity[c]
Alkyne-ML(38.8, 0.26)	−60	160, 166	59	0.05
25 wt% LML	−59	160, 166	59	0.03
50 wt% LML	−60	160	54	0.12
75 wt% LML	−61	156	55	0.06

[a] Determined during DSC measurement of first heating at 10 °C min^{-1}. [b] Determined as the peak of melting endotherm during DSC measurement of first heating at 10 °C min^{-1}. [c] Determined using the equation for degree of crystallinity = $\Delta H_m/(w_{PLLA} \times \Delta H_m^{\infty})$, where ΔH_m is the enthalpy of melting taken as the area under the melting endotherm during the first heat at 10 °C min^{-1}, ΔH_m^{∞} = 93 J g^{-1}, and w_{PLLA} is the weight fraction of PLLA.

The alkyne-ML(38.8, 0.26) and 25 wt% LML blend cold crystallized around 95 °C (peak temperature of cold crystallization exotherm). The 50 wt% LML blend showed a similar cold crystallization exothermic transition at 94 °C that was broader, while 75 wt% LML blends only cold crystalized at 110 °C with a broad peak shape and smaller amplitude. In the case of poly (ethylene glycol)-*block*-poly(L-lactide) star block copolymers (PEG-*b*-PLLA) with different architectures, the increased arm number of PEG-*b*-PLLA with the same molar masses of PLLA and PEG yielded reduced PLLA crystallinities, which was attributed to the reduced mobility of the star block copolymers.[43] Reduced cold crystallization kinetics have also been reported in poly(L-lactide)-*block*-poly(ethylene-*co*-ethylethylene) polymers with a multi-block architecture that was hypothesized to be due to the restricted chain mobility of bridges and loops.[44] In this context, the increase of cold crystallization temperature and broadening of cold crystallization peaks also reflects the presence of higher LML triblock content with reduced mobility in the 50 wt% and 75 wt% LML blends.

The linear viscoelastic properties of blends were also investigated using small amplitude oscillatory shear (SAOS) with frequency sweeps between −20 to 80 °C (Fig. 5 and Fig. S7†). Master curves were generated by horizontally shifting the data using a reference temperature of 20 °C. Effective PSAs should readily wet the substrate as a viscous liquid during a typical one-second bonding time, which requires the storage modulus (G') to be less than 0.3 MPa at 1 rad s^{-1} (Dahlquist criteria).[45] Moreover, the tan(δ) (*i.e.*, G''/G', where G'' is the loss modulus) should be 0.1–1.0 for sufficient cohesive strength and effective energy dissipation during debonding.[1]

The alkyne-ML(38.8, 0.26) and LML/ML blends showed a similar plateau G' in the high frequency range (*i.e.*, 2.1 MPa for alkyne-ML(38.8, 0.26), 1.5 MPa for 25 wt% LML blend, 2.3 MPa for 50 wt% LML blend and 3.1 MPa for 75 wt% LML blend at 100 rad s^{-1}). The value of the plateau modulus is dependent on the presence of entanglements in the rubbery matrix,[9,10] and PγMCL has a reported entanglement molar mass (M_e) of 2.9 kg mol^{-1}.[31] Therefore, alkyne-ML(38.8, 0.26) possesses a well-entangled rubbery matrix. While the formation of the LML triblock architecture does not increase the entanglement density in the blends, both LML and ML samples yielded similar plateau moduli in the high-frequency range (greater than 10^1 rad s^{-1}), akin to previous reports of SIS/SI blends.[10,15]

After solvent casting, the alkyne-ML(38.8, 0.26) (Fig. 5), 25 wt% LML (Fig. S7a†) and 50 wt% LML (Fig. S7b†) showed a relaxation at low frequencies that is more dissipative, evidenced by a high tan(δ). For instance, the tan(δ) at 1 rad s^{-1} for the ML diblock, 25 wt% LML blend, and 50 wt% LML blend were 0.47, 0.28, and 0.25, respectively. In contrast, the 75 wt% LML exhibited a low tan(δ) value of 0.09 at 1 rad s^{-1}, which is similar in magnitude to pure LML triblocks used as thermoplastic elastomers.[27,31] The increase of LML content decreased the tan(δ) values and enhanced the elasticity of the blends, while the dangling PγMCL ends of alkyne-ML(38.8, 0.26) could relax at longer relaxation times facilitating the drop of G' in the low frequency range producing more liquid-like, viscoelastic behavior. By tuning the LML content in the blends, the G' at 1 rad s^{-1} increased from 0.91 MPa for alkyne-ML(38.8, 0.26) to 0.94 MPa (25 wt% LML), 1.35 MPa (50 wt% LML), and 2.67 MPa (75 wt% LML). Therefore, these results indicate that tuning the molecular architecture in polyester block copolymer blends allows for convenient manipulation of

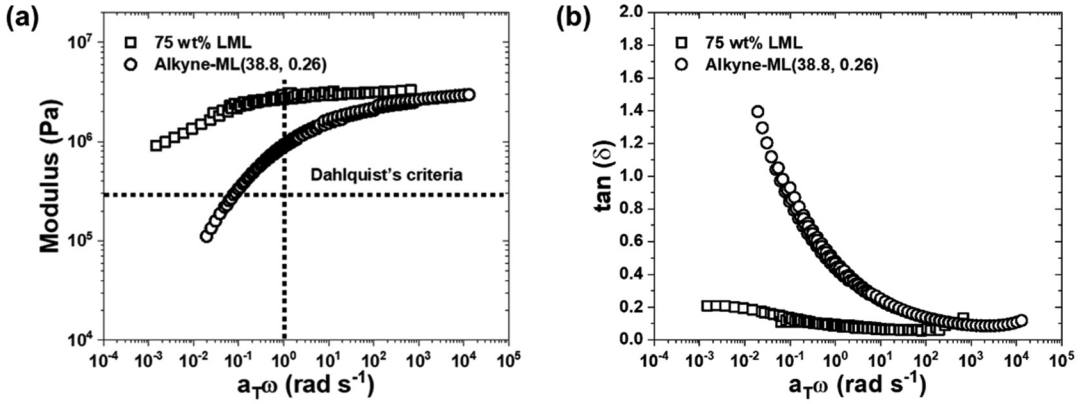

Fig. 5 Master curves for the (a) storage modulus (G') and (b) tan (δ) of alkyne-ML(38.8, 0.26) and 75 wt% LML blends after solvent casting. The Dahlquist criterion (G' = 0.3 MPa at 1 rad s^{-1}) is marked by dashed lines.

their viscoelastic properties. However, the G' at 1 rad s^{-1} of alkyne-ML(38.8, 0.26) and all LML/ML blends are all higher than the aforementioned Dahlquist criteria (*i.e.*, 0.3 MPa at 1 rad s^{-1}), highlighting the importance of adding tackifiers to enable more effective surface wetting for PSA applications.[1,6,11]

In addition to linear viscoelastic properties, the debonding of PSAs is impacted by their mechanical properties at large strain.[14,15] To understand the large-strain regime, the non-linear elastic behavior of alkyne-ML(38.8, 0.26) and LML/ML blends during the PSA debonding process were examined; 3 replicate samples for each formulation were subjected to tensile testing at an extension rate of 305 mm min^{-1} which is the same to the PSA peeling rate in the following 180° peel tests. Representative tensile data is shown in Fig. 6 and Table 3.

The pristine alkyne-ML(38.8, 0.26) contains no PγMCL bridging chains and accordingly is soft and has low ductility, with

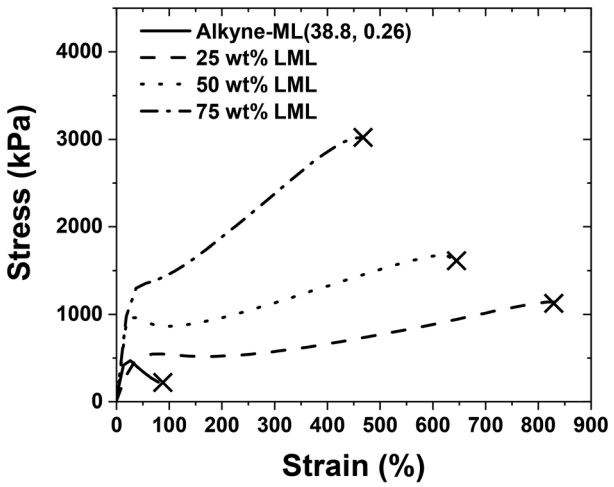

Fig. 6 Representative tensile data for alkyne-ML(38.8, 0.26) and LML/ML blends after solvent casting. Tensile tests were performed with an extension rate of 305 mm min^{-1}, with the break point indicated by ×.

Table 3 Tensile properties of alkyne-ML(38.8, 0.26) and LML/ML blends after solvent casting

Sample ID	δ_{Break}[a] (MPa)	ε_{Break}[a] (%)
Alkyne-ML(38.8, 0.26)	0.28 ± 0.05	77.2 ± 2.8
25 wt% LML	1.06 ± 0.05	853.3 ± 71.1
50 wt% LML	1.66 ± 0.09	649.3 ± 29.0
75 wt% LML	2.93 ± 0.12	457.0 ± 7.8

[a] Average values and standard deviations are calculated from tensile test of 3 replicates of each formulation extended at 305 mm min^{-1} until failure.

an average stress at break (δ_{Break}) of 0.28 ± 0.05 MPa and average strain at break (ε_{Break}) of 77.2% ± 2.8%. As a consequence, the lack of cohesive strength and ductility in the alkyne-ML(38.8, 0.26) is anticipated to compromise formation and extension of adhesive fibrils during the PSA debonding process, suggesting low peel strength and unfavorable cohesive failure (*i.e.*, leaving PSA residue on the substrate). The incorporation of 25 wt% LML in the blend significantly increased the tensile strength and ductility, produced an average δ_{Break} of 1.06 ± 0.05 MPa and an average ε_{Break} of 853.3% ± 71.1%. In the 25 and 50 wt% LML blends, strain softening was observed at intermediate strains, followed by strain hardening at high strain, which is similar to SIS/SI blends with a low SIS content.[14] Most SIS triblocks formed bridging PI midblocks without dangling ends, while the addition of SI diblocks of half molar mass linearly reduced the concentration of bridging PI chains in the SIS/SI blends.[46]

Further increase of LML content leads to enhanced tensile strengths, strain hardening effects with onsets at lower strain, and reduced ε_{Break} of 649.3% ± 29.0% for 50 wt% LML blends and 457% ± 7.8% for 75 wt% LML blends; these features resemble SIS/SI blends with high SIS triblock content or pure SIS triblocks.[14,15] By systematically tuning the LML content, the nonlinear mechanical properties of LML/ML blends were readily varied.

Adhesion properties

A renewable rosin ester tackifier (Sylvalite RE 80HP, solid powder at room temperature) was blended with alkyne-ML (38.8, 0.26) and LML/ML blends to dilute entanglements in the PγMCL rubbery matrix and promote interfacial adhesion with the substrate. The mass fraction of tackifier was kept at 20 wt% in the PSAs to avoid phase separation of the tackifier and PγMCL phase at high tackifier loading observed in a previous study.[27] The PSAs were prepared by blending all compounds in chloroform and solvent casting using a wire wound rod on poly(ethylene terephthalate) (PET) film (details in ESI†) and drying, resulting in transparent PSA films with thickness around 80 μm. The adhesion properties of the PSAs were then characterized in terms of their peel strength, failure mode in peel adhesion tests and shear resistance time under an applied shear stress of about 15.2 kPa on stainless steel substrates (Fig. 7 and Table 4). Details of experimental conditions and parameters can be found in the ESI.†

PSAs from tackified alkyne-ML(38.8, 0.26) showed a peel strength of 1.23 ± 0.15 N cm^{-1} and cohesive failure in the 180° peel adhesion test, leaving adhesive residue on the stainless-steel substrate (Fig. 7a, leftmost image). With increasing LML content, the peel adhesion failure mode shifted from cohesive failure to more preferred adhesive failure, without leaving any adhesive residue on the substrate after peeling (Fig. 7a, middle and rightmost image). Without LML triblock bridging, alkyne-ML(38.8, 0.26)-based PSAs lacked cohesive strength to maintain their structural integrity during the debonding process; this is also reflected by the low shear resistance (*i.e.*, 56 ± 10 min), highlighting an opportunity for improvement by addition of LML triblock. The addition of LML in the tackified PSAs increased the shear resistance (Fig. 7b and Table 4) (*e.g.*, 1497 ± 273 min for 75 wt% LML in LML/ML blends). We posit the increased LML triblock content established an increased concentration of elastic interconnecting PγMCL midblock bridging segments, allowing the PSA to maintain microstructural integrity ultimately leading to enhanced shear resistance and change in peel adhesion failure mode.

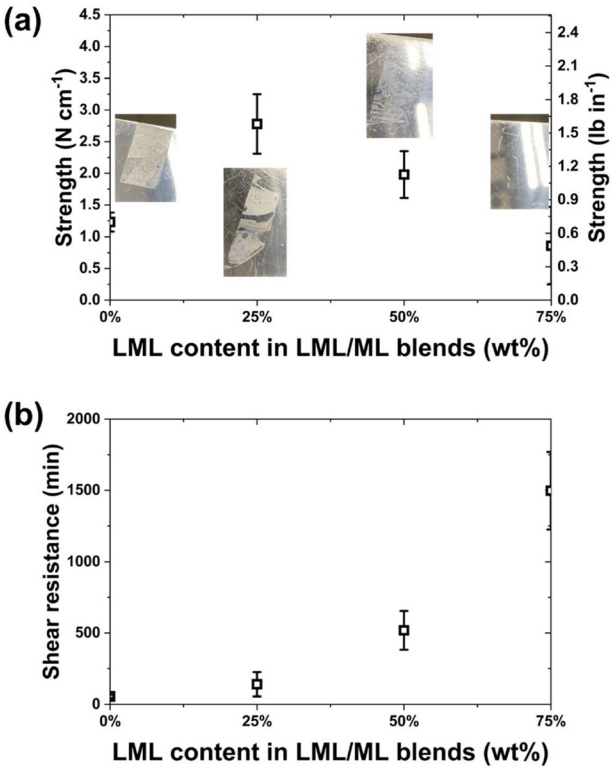

Fig. 7 (a) 180° peel adhesion properties and (b) shear resistance properties on stainless steel substrates of alkyne-ML(38.8, 0.26) and LML/ML blends after solvent casting with additional 20 wt% tackifier. All of the 180° peel adhesion tests were performed at the rate of 305 mm min^{-1}. Inserted digital images in (a) show the stainless steel substrate surfaces after the 180° peel adhesion tests.

Table 4 Adhesion properties of PSA from alkyne-ML(38.8, 0.26) and LML/ML blends after solvent casting with additional 20 wt% tackifier

Sample ID	Peel strength (N cm^{-1})	Peel adhesion failure mode	Shear (min)
Alkyne-ML (38.8, 0.26)	1.23 ± 0.15	Cohesive failure	56 ± 10
25 wt% LML	2.78 ± 0.47	Cohesive failure	140 ± 85
50 wt% LML	1.98 ± 0.37	Cohesive/adhesive failure	518 ± 163
75 wt% LML	0.86 ± 0.61	Adhesive failure	1497 ± 273

The relationship between LML content in the PSA formulations and peel strength is shown in (Fig. 7a). Compared to tackified PSA using pure ML, the tackified PSA with 25 wt% LML showed an increase in peel strength to 2.78 ± 0.47 N cm^{-1}. The peel strength then monotonically decreased with more LML (1.98 ± 0.37 N cm^{-1} for 50 wt% LML and 0.86 ± 0.61 N cm^{-1} for 75 wt% LML) as the PSA became more elastic and thus was less prone to wetting and establishing good contact with the substrate. At low LML contents, the LML/ML blends maintained dissipative characteristics from pure ML diblocks and possess low G' that promotes interfacial adhesion with the substrate during PSA bonding. As indicated by the high ductility during tensile testing, the presence of LML triblocks enhanced the cohesive strength of the PSA and likely enabled effective fibril extension during PSA debonding. Collectively, the sufficient interfacial adhesion and enhanced cohesive strength contributed to improved peel strength and a transition to adhesive failure. However, in the case of 75 wt% LML, the high G' and low tan (δ) simultaneously reduced the interfacial adhesion, likely due to poor wetting, leading to decreased peel strength, which is similar to the case of pure LML triblocks and 20 wt% tackifier in our previous study (*i.e.*, 0.35 ± 0.02 N cm^{-1}).[27] Therefore, by systematically manipulating the LML triblock content in the blends, the adhesion properties of tackified PSA can be readily tuned.

To further evaluate the adhesion properties, the tackified PSAs were subjected to a two-step annealing process (*i.e.*, first

above the melting temperature of PLLA at 170 °C for 60 minutes and second at 100 °C to cold-crystallize the PLLA).[27] The shear resistance of the PSAs did not significantly change (Fig. S9 and Table S3†). Similar to our previous results, formation of enhanced microphase separation and semicrystalline PLLA domains contributed to substantially enhanced peel strengths after annealing (Fig. S10 and Table S3†). For instance, the peel strengths of tackified PSAs were increased to 2.37 ± 0.48 N cm^{-1} (alkyne-ML(38.8, 0.26)), 4.11 ± 0.16 N cm^{-1} (25 wt% LML), 3.66 ± 0.33 N cm^{-1} (50 wt% LML) and 1.53 ± 0.28 N cm^{-1} (75 wt% LML), which is comparable to commercial products.[26] This demonstration is encouraging as it is more relevant to high speed accelerated solvent drying processes or hot melt PSA processing.

We explored the potential generalizability of this blending approach in a more polymer manufacturing friendly manner using two different methods to prepare LML/ML blends with 50 wt% LML. First, LML(74.0, 0.25) and ML(37.5, 0.22) were synthesized separately by sequential ROTEPs with similar compositions and block length by using 1,4-benzenedimethanol and benzyl alcohol as initiator, respectively. Molecular characteristics of LML(74.0, 0.25) and ML(37.5, 0.22) can be found in Table S2.† The separately as-prepared LML(74.0, 0.25) and ML (37.5, 0.22) were then dissolved in chloroform to form a LML/ML blend with 50 wt% LML. In a separate experiment, a mixture of 1,4-benzenedimethanol and benzyl alcohol initiators were added together in a 1 to 2 molar ratio to form a LML/ML blend with 50 wt% LML by simultaneous sequential ROTEP. This approach should theoretically yield ML and LML of similar compositions and block length. The molar mass of PγMCL was controlled by the molar ratio of monomer to hydroxyl group of the initiators (250 to 1) and a conversion over 95%, producing roughly 30 kg mol^{-1} PγMCL, which is similar to the length of the PγMCL block in the other two methods. The f_{PLLA} was controlled by the amount of L-lactide monomer added to the reaction, and running to high monomer conversion in the second ROTEP step. The molecular characteristics of LML/ML blends synthesized from the third method can be found in Table S4.† However, the precise LML content in the blend could not be readily determined due to the unimodal peak shape in the SEC trace (Fig. S11†). The solvent-cast PSAs with additional 20 wt% tackifier of these LML/ML blends were prepared following the same procedure noted above and the 180° peel test results were summarized in Table S5.†

Under the same processing conditions and with the same amount of tackifier, the peel strengths of PSAs from these two routes (*i.e.*, 1.65 ± 0.25 N cm^{-1} from post-synthesis blending and 1.21 ± 0.52 N cm^{-1} from simultaneous polymerization) were not statistically different from that of PSAs prepared from LML/ML blends synthesized by the azide–alkyne coupling synthetic strategy (Table S5†), and all PSAs failed by adhesive failure. Regardless of preparation method, PSAs from LML/ML blends with optimized LML contents should manifest similar, improved adhesion properties compared to that of pure LML triblock or ML diblock copolymers.

Hydrolytic degradation

The hydrolytic degradation of as-prepared PSAs was performed in 1 M NaOH aqueous solution at 45 °C and monitored by total organic carbon (TOC) analysis to quantify hydrolyzed products that leached into the aqueous media (Fig. 8 and Fig. S12†). Pristine LML triblocks were found to be completely degradable *via* hydrolytic degradation under the same conditions,[27] by enzymatic catalysis,[23] or under simulated industrial composting conditions.[24] Under basic conditions, the transparent PSAs turned opaque in 1 day and detached from the PET substrate after 10 days, forming white particles suspended in solution. As shown in Fig. 8, the hydrolytic degradation of tackified PSAs from LML/ML blends of 50 wt% LML led to a rapid increase in TOC values during the first 7 days and reached plateau values around 80% degradation after 15 days, affirming the excellent hydrolytic degradability of LML-based polyester block copolymer blends under basic conditions. Increasing the LML content in the blend did not change the TOC plateau values (Fig. S12†), but slightly reduced the degradation kinetics. Since all PSAs afforded similar compositions and were degraded under the same process, the slightly slower degradation kinetics were possibly a result of the longer time that the higher molar mass LML needed to be degraded into water-soluble or dispersible products. In a previous study, PSAs from tackified LML triblocks also experienced incomplete degradation under these conditions,[27] which was attributed to the lack of hydrolytic degradability of the rosin ester tackifier.[47] Clearly, the LML/ML blends studied here exhibited high levels of hydrolytic degradability while also affording enticing tunability through molecular architecture and blend composition for optimizing their adhesion properties.

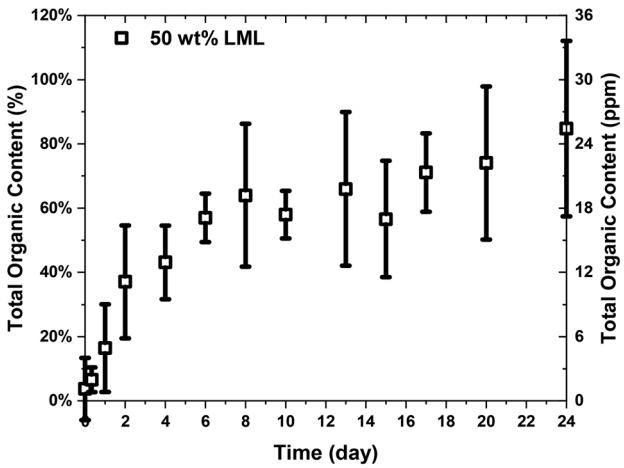

Fig. 8 Hydrolytic degradation of solvent cast 20 wt% tackified LML/ML blend PSAs with 50 wt% LML in 1 M NaOH aqueous solution at 45 °C. The total organic carbon (TOC) content is the ratio of measured organic carbon in the aqueous solutions to the theoretical total carbon content of the blends with tackifier. The data points and error bars represent average and range for triplicate experiments, respectively.

Conclusion

LML/ML all-aliphatic polyester block copolymer blends were successfully prepared by combining sequential ROTEP to form ML diblock copolymers with a terminal alkyne and then coupling a fraction of the parent diblocks by copper-catalyzed alkyne–azido cycloaddition. The LML content in the blends after coupling could be tailored from 25 wt% to 75 wt% by tuning the stoichiometric ratio of bifunctional azido linker to alkyne ended ML diblock copolymer. This provided a convenient strategy to prepare LML/ML blends with the same composition and block length, but distinctive molecular architectures *via* azide–alkyne coupling. The effect of LML blend content on the microstructure, crystallinity, thermal and mechanical properties of the blends were systematically investigated. PSAs were formulated by blending with 20 wt% of a renewable tackifier, and the application of these LML/ML blends as PSAs showed widely tailorable adhesion properties that correlated to the LML content. With 50 wt% of LML in the LML/ML blends, the tackified PSAs exhibited simultaneously sufficient interfacial adhesion and improved cohesive strength owing to the balance of dangling and bridging PγMCL blocks in the rubbery matrix. After solvent casting, the PSA afforded a 1.98 ± 0.37 N cm^{-1} peel strength, desired adhesive failure mode in 180° peel tests and a shear resistance of 518 ± 163 minutes. After an additional two-step annealing process, the peel strength of this tackified PSA of the same composition was further improved to 3.66 ± 0.33 N cm^{-1}, which is comparable to many commercial products, with no significant difference in shear strength. It was shown that this blending approach is potentially generalizable *via* other more polymer manufacturing friendly approaches, such as post-synthesis blending and simultaneous polymerization with mixtures of different initiators. The high hydrolytic degradability of these LML/ML blends were demonstrated in 1 M NaOH aqueous solution at 45 °C suggesting promising sustainability prospects afforded by the ester linkages in the backbone. In summary, our results indicate the molecular architecture of polyester block copolymers allows for ready engineering of their properties for PSA applications with enticing renewability, degradability and competitive performance.

Conflicts of interest

There are no conflicts to declare.

Data availability

Accompanying this manuscript is a ESI† file detailing experimental procedures, materials, and sample characterizations. The primary data files are archived with the Data Repository for the University of Minnesota and accessible *via* **https://doi.org/10.13020/qqdx-g304**.

Acknowledgements

This work was supported by the Avery Dennison Corporation with support from the National Science Foundation Center for Sustainable Polymers at the University of Minnesota, which is a National Science Foundation-supported Center for Chemical Innovation (CHE-1901635). NMR research reported in this publication was supported by the Office of the Vice President of Research, College of Science and Engineering, and the Department of Chemistry at the University of Minnesota. The authors would like to thank Dr. Yoon-Jung Jang, Brenden Hoehn, Daniel Krajovic, Dr. Shuquan Cui, Dr. Alex Nyarko, Dr. Tom Ribelli, Dr. Eric Bartholomew and Keisha Ross for helpful discussions and assistance in experiment design.

References

1 C. Creton, Pressure-Sensitive Adhesives: An Introductory Course, *MRS Bull.*, 2003, **28**(6), 434–439.
2 A. Zosel, Adhesion and tack of polymers: Influence of mechanical properties and surface tensions, *Colloid Polym. Sci.*, 1985, **263**(7), 541–553.
3 A. J. Crosby and K. R. Shull, Adhesive failure analysis of pressure-sensitive adhesives, *J. Polym. Sci., Part B: Polym. Phys.*, 1999, **37**(24), 3455–3472.
4 M. M. Feldstein and R. A. Siegel, Molecular and nanoscale factors governing pressure-sensitive adhesion strength of viscoelastic polymers, *J. Polym. Sci., Part B: Polym. Phys.*, 2012, **50**(11), 739–772.
5 T. R. Ewert, A. M. Mannion, M. L. Coughlin, C. W. Macosko and F. S. Bates, Influence of rheology on renewable pressure-sensitive adhesives from a triblock copolymer, *J. Rheol.*, 2018, **62**(1), 161–170.
6 C. Galán, C. A. Sierra, J. M. G. Fatou and J. A. Delgado, A hot-melt pressure-sensitive adhesive based on styrene–butadiene–styrene rubber. The effect of adhesive composition on the properties, *J. Appl. Polym. Sci.*, 1996, **62**(8), 1263–1275.
7 A. E. O'Connor and C. W. Macosko, Melt versus solvent coating: Structure and properties of block–copolymer-based pressure-sensitive adhesives, *J. Appl. Polym. Sci.*, 2002, **86**(13), 3355–3367.
8 G. Kraus, F. B. Jones, O. L. Marrs and K. W. Rollmann, Morphology and Viscoelastic Behavior of Styrene-Diene Block Copolymers in Pressure Sensitive Adhesives, *J. Adhes.*, 1976, **8**(3), 235–258.
9 G. Kraus and K. W. Rollmann, The entanglement plateau in the dynamic modulus of rubbery styrene–diene block copolymers. Significance to pressure-sensitive adhesive formulations, *J. Appl. Polym. Sci.*, 1977, **21**(12), 3311–3318.
10 F. X. Gibert, G. Marin, C. Derail, A. Allal and J. Lechat, Rheological properties of hot melt pressure-sensitive adhesives based on styrene–isoprene copolymers. Part 1: A rheological model for [sis-si] formulations, *J. Adhes.*, 2003, **79**(8–9), 825–852.

11 M. Sasaki, K. Fujita, M. Adachi, S. Fujii, Y. Nakamura and Y. Urahama, The effect of tackifier on phase structure and peel adhesion of a triblock copolymer pressure-sensitive adhesive, *Int. J. Adhes. Adhes.*, 2008, **28**(7), 372–381.
12 M. A. Droesbeke, R. Aksakal, A. Simula, J. M. Asua and F. E. Du Prez, Biobased acrylic pressure-sensitive adhesives, *Prog. Polym. Sci.*, 2021, **117**, 101396.
13 Y. Nakamura, M. Adachi, Y. Kato, S. Fujii, M. Sasaki, Y. Urahama and S. Sakurai, Effects of Polystyrene Block Content on Morphology and Adhesion Property of Polystyrene Block Copolymer, *J. Adhes. Sci. Technol.*, 2011, **25**(8), 869–881.
14 C. Creton, G. Hu, F. Deplace, L. Morgret and K. R. Shull, Large-Strain Mechanical Behavior of Model Block Copolymer Adhesives, *Macromolecules*, 2009, **42**(20), 7605–7615.
15 A. Roos and C. Creton, Effect of the Presence of Diblock Copolymer on the Nonlinear Elastic and Viscoelastic Properties of Elastomeric Triblock Copolymers, *Macromolecules*, 2005, **38**(18), 7807–7818.
16 M. Sasaki, M. Adachi, Y. Kato, S. Fujii, Y. Nakamura, Y. Urahama and S. Sakurai, Adhesion property and morphology of styrene triblock/diblock copolymer blends, *J. Appl. Polym. Sci.*, 2010, **118**(3), 1766–1773.
17 R. Geyer, J. R. Jambeck and K. L. Law, Production, use, and fate of all plastics ever made, *Sci. Adv.*, 2017, **3**(7), e1700782.
18 M. Park, S.-J. Hong, N.-K. Kim, J. Shin and Y.-W. Kim, Vegetable Oil-Derived Polyamide Multiblock Copolymers toward Chemically Recyclable Pressure-Sensitive Adhesives, *ACS Sustainable Chem. Eng.*, 2023, **11**(27), 10095–10107.
19 C. Xu, L. Wang, Y. Liu, H. Niu, Y. Shen and Z. Li, Rapid and Controlled Ring-Opening (Co)Polymerization of Bio-Sourced Alkyl-δ-Lactones To Produce Recyclable (Co) Polyesters and Their Application as Pressure-Sensitive Adhesives, *Macromolecules*, 2023, **56**(15), 6117–6125.
20 K. R. Albanese, Y. Okayama, P. T. Morris, M. Gerst, R. Gupta, J. C. Speros, C. J. Hawker, C. Choi, J. R. de Alaniz and C. M. Bates, Building Tunable Degradation into High-Performance Poly(acrylate) Pressure-Sensitive Adhesives, *ACS Macro Lett.*, 2023, **12**(6), 787–793.
21 R. Auras, B. Harte and S. Selke, An Overview of Polylactides as Packaging Materials, *Macromol. Biosci.*, 2004, **4**(9), 835–864.
22 D. J. Lundberg, D. J. Lundberg, M. A. Hillmyer and P. J. Dauenhauer, Techno-economic Analysis of a Chemical Process To Manufacture Methyl-ε-caprolactone from Cresols, *ACS Sustainable Chem. Eng.*, 2018, **6**(11), 15316–15324.
23 G. X. De Hoe, M. T. Zumstein, B. J. Tiegs, J. P. Brutman, K. McNeill, M. Sander, G. W. Coates and M. A. Hillmyer, Sustainable Polyester Elastomers from Lactones: Synthesis, Properties, and Enzymatic Hydrolyzability, *J. Am. Chem. Soc.*, 2018, **140**(3), 963–973.
24 L. Reisman, A. Siehr, J. Horn, D. C. Batiste, H. J. Kim, G. X. De Hoe, C. J. Ellison, W. Shen, E. M. White and M. A. Hillmyer, Respirometry and Cell Viability Studies for Sustainable Polyesters and Their Hydrolysis Products, *ACS Sustainable Chem. Eng.*, 2021, **9**(7), 2736–2744.
25 J. Shin, M. T. Martello, M. Shrestha, J. E. Wissinger, W. B. Tolman and M. A. Hillmyer, Pressure-Sensitive Adhesives from Renewable Triblock Copolymers, *Macromolecules*, 2011, **44**(1), 87–94.
26 H. J. Kim, K. Jin, J. Shim, W. Dean, M. A. Hillmyer and C. J. Ellison, Sustainable Triblock Copolymers as Tunable and Degradable Pressure Sensitive Adhesives, *ACS Sustainable Chem. Eng.*, 2020, **8**(32), 12036–12044.
27 S. Liang, D. M. Krajovic, B. D. Hoehn, C. J. Ellison and M. A. Hillmyer, Engineering Aliphatic Polyester Block Copolymer Blends for Hydrolytically Degradable Pressure Sensitive Adhesives, *ACS Appl. Polym. Mater.*, 2024, **7**(3), 1411–1420.
28 J. L. Daristotle, M. Erdi, L. W. Lau, S. T. Zaki, P. Srinivasan, M. Balabhadrapatruni, O. B. Ayyub, A. D. Sandler and P. Kofinas, Biodegradable, Tissue Adhesive Polyester Blends for Safe, Complete Wound Healing, *ACS Biomater. Sci. Eng.*, 2021, **7**(8), 3908–3916.
29 J. L. Daristotle, S. T. Zaki, L. W. Lau, O. B. Ayyub, M. Djouini, P. Srinivasan, M. Erdi, A. D. Sandler and P. Kofinas, Pressure-Sensitive Tissue Adhesion and Biodegradation of Viscoelastic Polymer Blends, *ACS Appl. Mater. Interfaces*, 2020, **12**(14), 16050–16057.
30 S. Liffland and M. A. Hillmyer, Enhanced Mechanical Properties of Aliphatic Polyester Thermoplastic Elastomers through Star Block Architectures, *Macromolecules*, 2021, **54**(20), 9327–9340.
31 A. Watts, N. Kurokawa and M. A. Hillmyer, Strong, Resilient, and Sustainable Aliphatic Polyester Thermoplastic Elastomers, *Biomacromolecules*, 2017, **18**(6), 1845–1854.
32 S. A. da Silva, C. L. Marques and N. S. M. Cardozo, Composition and Performance of Styrene-Isoprene-Styrene (SIS) and Styrene-Butadiene-Styrene (SBS) Hot Melt Pressure Sensitive Adhesives, *J. Adhes.*, 2012, **88**(2), 187–199.
33 L.-J. Zhang, B.-T. Dong, F.-S. Du and Z.-C. Li, Degradable Thermoresponsive Polyesters by Atom Transfer Radical Polyaddition and Click Chemistry, *Macromolecules*, 2012, **45**(21), 8580–8587.
34 B. Parrish, R. B. Breitenkamp and T. Emrick, PEG- and Peptide-Grafted Aliphatic Polyesters by Click Chemistry, *J. Am. Chem. Soc.*, 2005, **127**(20), 7404–7410.
35 Y. Nagao and A. Takasu, "Click polyester": Synthesis of polyesters containing triazole units in the main chain via safe and rapid "click" chemistry and their properties, *J. Polym. Sci., Part A: Polym. Chem.*, 2010, **48**(19), 4207–4218.
36 E. J. O'Neil, K. M. DiVittorio and B. D. Smith, Phosphatidylcholine-Derived Bolaamphiphiles via Click Chemistry, *Org. Lett.*, 2007, **9**(2), 199–202.
37 D. M. Krajovic, G. Haugstad and M. A. Hillmyer, Crystallinity-Independent Toughness in Renewable Poly(l-

lactide) Triblock Plastics, *Macromolecules*, 2024, **57**(6), 2818–2834.

38 R. Abu Bakar, Y. Li, O. P. Hewitson, P. J. Roth and J. L. Keddie, Azide Photochemistry in Acrylic Copolymers for Ultraviolet Cross-Linkable Pressure-Sensitive Adhesives: Optimization, Debonding-on-Demand, and Chemical Modification, *ACS Appl. Mater. Interfaces*, 2022, **14**(26), 30216–30227.

39 T. Doi, H. Takagi, N. Shimizu, N. Igarashi and S. Sakurai, Effects of drying temperature in solution coating process on microphase-separated structures in coated layers of pressure-sensitive adhesive composed of di- and triblock copolymer blends as revealed by small-angle X-ray scattering, *Polymer*, 2019, **170**, 211–221.

40 Y. Mori, L. S. Lim and F. S. Bates, Consequences of Molecular Bridging in Lamellae-Forming Triblock/Pentablock Copolymer Blends, *Macromolecules*, 2003, **36**(26), 9879–9888.

41 Y. Matsushita, K. Mori, R. Saguchi, Y. Nakao, I. Noda and M. Nagasawa, Molecular weight dependence of lamellar domain spacing of diblock copolymers in bulk, *Macromolecules*, 1990, **23**(19), 4313–4316.

42 J. Zhang, K. Tashiro, H. Tsuji and A. J. Domb, Disorder-to-Order Phase Transition and Multiple Melting Behavior of Poly(l-lactide) Investigated by Simultaneous Measurements of WAXD and DSC, *Macromolecules*, 2008, **41**(4), 1352–1357.

43 D. Zhou, J. Shao, G. Li, J. Sun, X. Bian and X. Chen, Crystallization behavior of PEG/PLLA block copolymers: Effect of the different architectures and molecular weights, *Polymer*, 2015, **62**, 70–76.

44 T. R. Panthani and F. S. Bates, Crystallization and Mechanical Properties of Poly(l-lactide)-Based Rubbery/Semicrystalline Multiblock Copolymers, *Macromolecules*, 2015, **48**(13), 4529–4540.

45 C. A. Dahlquist and R. Patrick, Treatise on adhesion and adhesives. in: *Pressure-sensitive adhesives*, Marcel Dekker, Inc, New York, 1969, pp. 219–260.

46 K. C. Daoulas, D. N. Theodorou, A. Roos and C. Creton, Experimental and Self-Consistent-Field Theoretical Study of Styrene Block Copolymer Self-Adhesive Materials, *Macromolecules*, 2004, **37**(13), 5093–5109.

47 N. H. Sahu, P. M. Mandaogade, A. M. Deshmukh, V. S. Meghre and A. K. Dorle, Biodegradation Studies of Rosin-Glycerol Ester Derivative, *J. Bioact. Compat. Polym.*, 1999, **14**(4), 344–360.

